Modeling of Microcellular Short Fiber Reinforced Plastics for Pedestrian Safety Analysis

Mats Landervik[1], Simon Gastl[2], Ulf Westberg[3]

[1]DYNAmore Nordic
[2]Borealis Polyolefine GmbH
[3]Volvo Car Corporation

1 Introduction

For efficient vehicle development there is a strive to reduce prototypes and shorten development times which leads to the need to rely on CAE methods for continuous evaluation of product performance. This puts demands on the CAE methods, not only in terms of predictability but also in terms of how well they integrate in the development process. Model preparation, material characterization and computational costs are important aspects for successful integration. New materials and production methods are other drivers for CAE method development as current methods may not be adequate. Short fiber reinforced polymers (SFRP) have found their way into more automotive applications in recent years. Weight, the geometrical possibilities, part production cycle times and cost are some of the potential benefits. The injection molding process, however, leads to an inhomogeneous distribution of fiber orientation throughout a part. As the fiber orientation distribution has significant impact on the mechanical properties it causes anisotropy and spatial variations of the material response. This paper addresses the modeling of an SFRP part which is produced by gas assisted injection molding leading to a porous, microcellular, material consisting of three phases, i.e. matrix-, fiber- and pore phases.

DIGIMAT [1] is a software suite which is commonly used for the modeling of SFRP in various applications, various types of CAE analyses and with various FE solvers. The DIGIMAT material model is available in LS-DYNA through the user material interface. Alternative material models in LS-DYNA are *MAT_157 and *MAT_215 which feature dependency of the local fiber orientation being mapped from injection simulation [5-7]. Using DIGIMAT for SFRP in crash analysis was previously reported in [2-4]. What is new in the present paper is the pore phase that adds to the modeling complexity. The material concerned in this paper is Borealis Fibremod GD302HP, a 30% glass fiber reinforced polypropylene compound, which was characterized as described in Section 3. The characterization, however, is done for the non-porous material and it is assumed that the material will have similar stress contribution from the solid phases in the porous material. The effect of porosity on failure is less certain. Studies on the effect of porosity on the mechanical response are found for PPGF20 [9] and PA66GF30 [10]. In [9], bending tests show lower failure strain for increasing porosity and in [10], tensile tests show an increase in failure strain in the dominant fiber direction and a decrease in the transverse direction. DIGIMAT has the feature to scale the failure strains as a function of the porosity. However, for the present paper it is assumed that the effect is small, and it is therefore neglected.

The aim of this paper is to validate the applied modeling methodology through testing and simulation of drop tower impacts (Section 5). However, since the methodology relies additionally on the prediction of fiber orientation and porosity from process simulation, efforts to validate the prediction are done (Section 4).

2 Application

The component in the present study is the combined bracket in the front structure of the Volvo models S90 and V90, Fig. 1. The response of this component has significant impact on the injury values measured in the legform to bumper tests used for legal compliance and rating, e.g. Euro NCAP [11-13]. In order to design a car structure that will meet all requirements, achieve top safety rating and provide best possible real-life safety, reliable CAE predictions are essential. For a component like the combined bracket, we need to closely predict the rate dependent force response as well as failure since that will have high influence on the forces on the tibia and knee in the lower leg test.

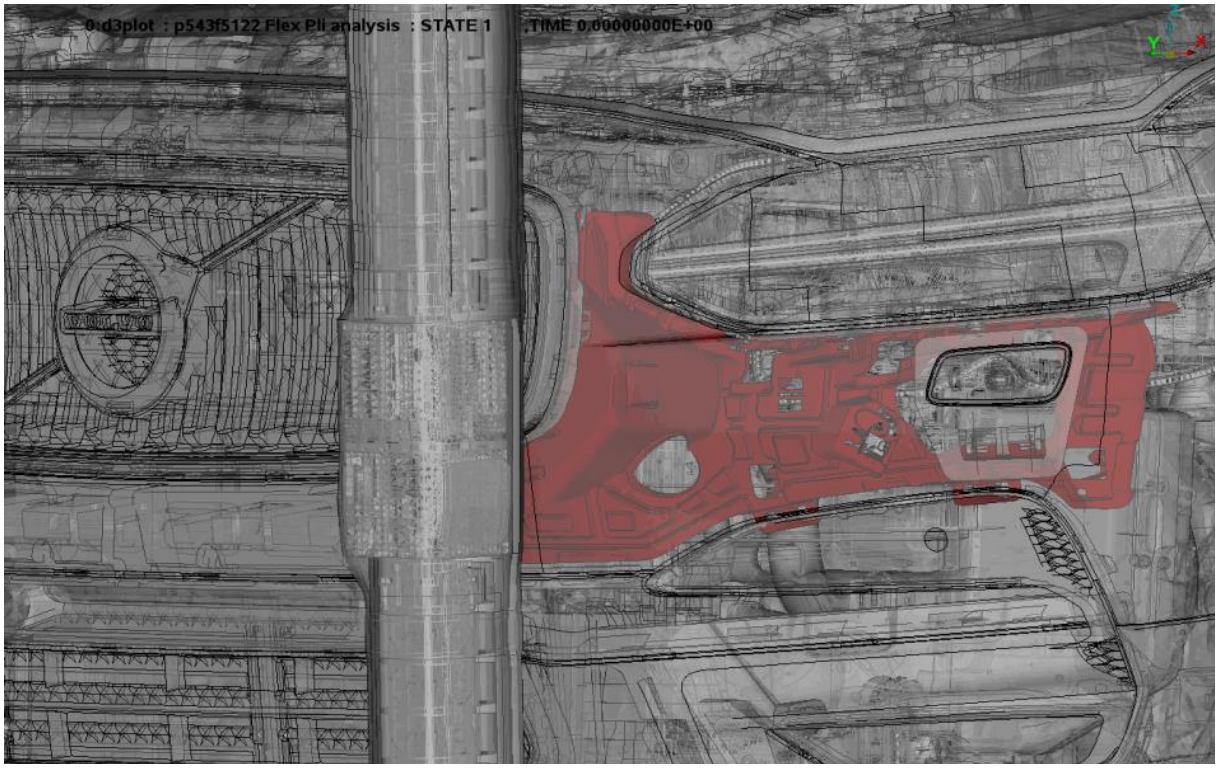

Fig.1: The combined bracket (red) in the front structure of the Volvo models S90 and V90 in an FE simulation of a lower leg pedestrian Euro NCAP rating test [11-13].

3 Material model and characterization

The mechanical performance of short fiber reinforced polymeric composites strongly depends on the fiber orientation distribution. Proper prediction of the part performance under service life conditions necessitates characterizing the influence of the orientation on the material behaviour. Therefore, the Borealis Glass-Fiber-Tool (Fig.2) was introduced to allow for advanced characterization of fiber-reinforced materials. The tool has a thickness of 2 mm and specimens with very distinct fibre-orientations (0°, 45° and 90°).

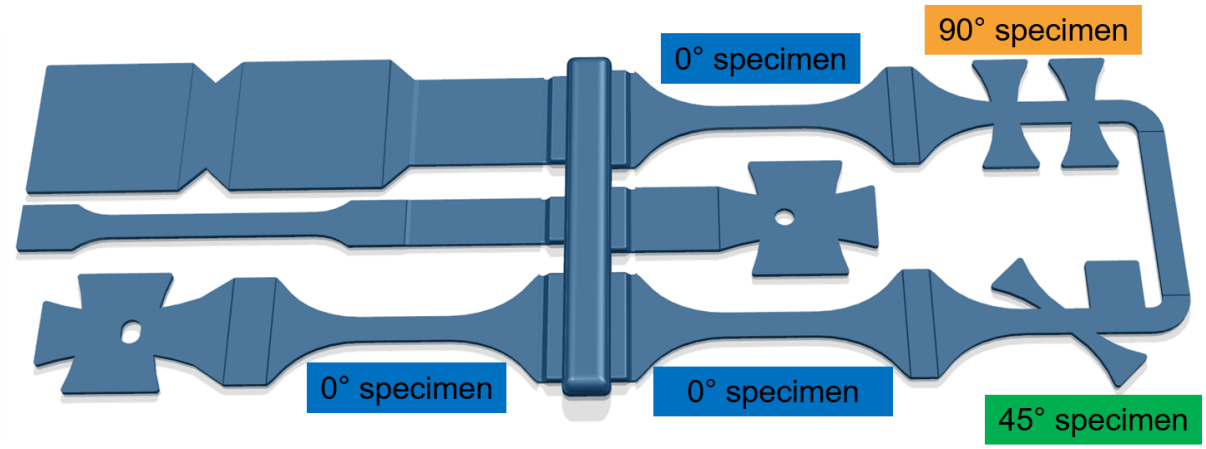

Fig.2: The Borealis GF-Tool.

To gain information about the microstructure of the specimens, computed tomography (CT) investigations were carried out using sub-µm-CT. Fig. 3 shows the CT-device, a representative measurement volume and a resulting fiber orientation tensor.

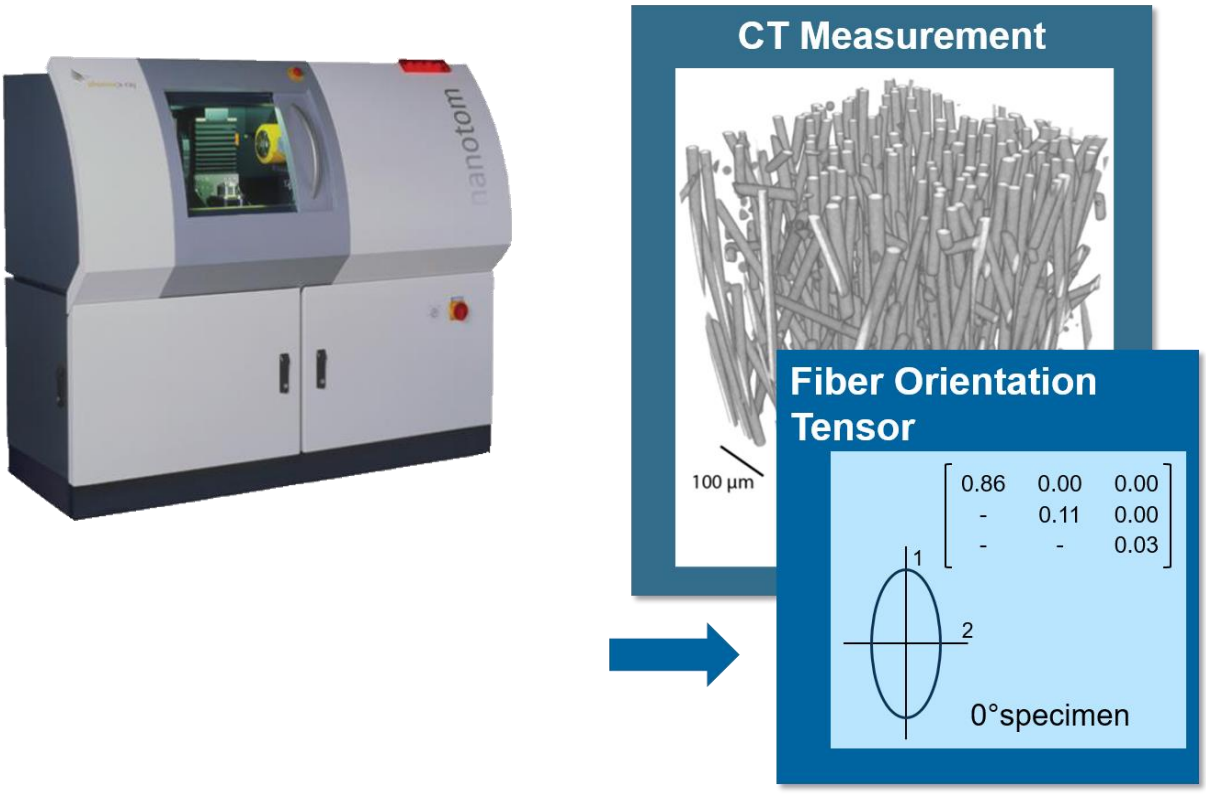

Fig.3: Nanotom®- laboratory device.

Tensile tests, using Digital Image Correlation (DIC) at different strain rates (0.001, 0.01, 0.1, 1, 10 and 100) were conducted. The optical strain measurement (Fig. 4) allows the gathering of information about the local strain at break for different fiber orientations.

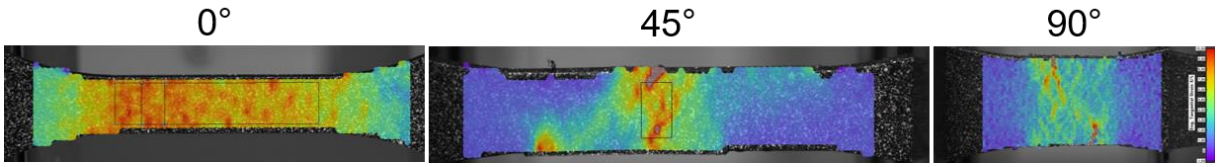

Fig.4: Optical strain measurements of the GF-Tool specimens with different fiber orientations (0°, 45° and 90°).

With knowledge about the fiber orientation and the results of the mechanical testing, a reverse engineering routine to identify the composite behaviour was used and the resulting material model is shown in Fig. 5.

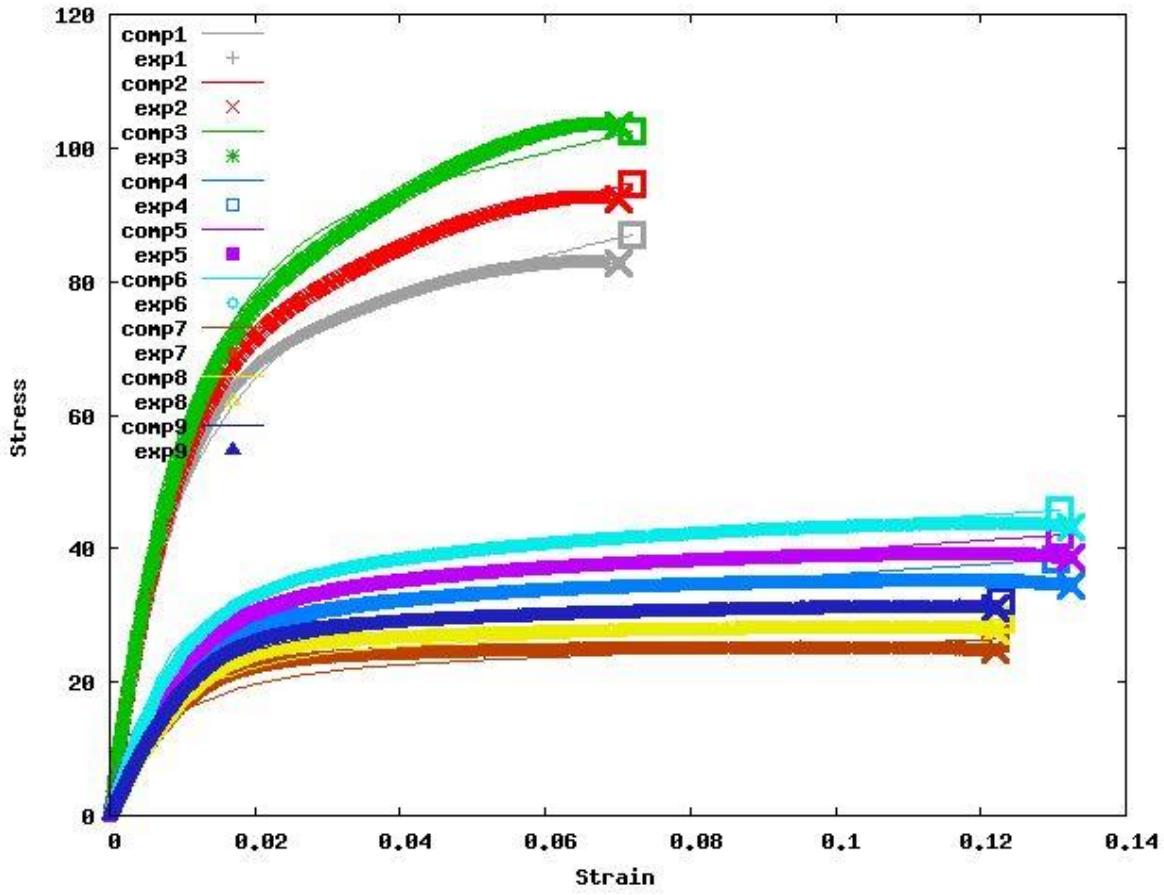

Fig.5: Calibrated material model. The figure shows the experiments vs. material model for three different fiber orientations (0°, 45° and 90°) at three different strain rates (1, 10, 100).

4 Prediction and validation of fiber orientation and porosity

Injection molding simulations are performed to feed the Digimat material model with local fiber orientation tensor and porosity. The simulation was done in Moldflow by the component supplier Plastal. To facilitate the mapping of data to the mesh in the impact simulation, the same mesh is used for the injection simulation with the only difference that each quad element is first split into four triangles to reach the same resolution as for an LS-DYNA type 16 quad element. It should be noted that alternatively a solid tetrahedron mesh may be used in Moldflow. It is possible that a 3D simulation may, due to the potentially higher geometrical accuracy, provide better estimation of fiber orientation and porosity. It is indeed possible to map from solid to shell mesh. The geometrical differences between a shell and solid model will however give a lower accuracy of the mapping. Shell Moldflow simulation with a high resolution in the thickness direction is chosen for its smaller model size compared to a solid simulation as well as making the mapping simpler.

In order to validate the Moldflow predictions, components were sent to North Star Imaging Europe in France where six 10*10 mm specimens were cut from the plane where the failure occurs in the drop tests (Section 5). X-ray 3D computed tomography were performed on the specimens followed by the identification of phases and quantification of the components of the fiber orientation, the fiber volume fraction and the pore volume fraction for the number of 9*9*23–9*9*25 cells with the in-plane dimension of 1*1 mm and a thickness of 0.1 mm. In Fig. 6 the first eigenvector of the orientation tensor is drawn for the second layer close to the surface for Moldflow prediction and CT scan. We see that the vectors coincide well for the samples 3 and 4 where the melt flow direction is stable. The melt inlet is in the top surface of the “cone” (see e.g. Fig. 8) which is on a higher level in the x-direction. Thus, the melt flows down the sides of the cone to reach the sample surface leading to changes in flow direction close to the samples 1, 2, 5 and 6. It is assumed that the applied resolution of the Moldflow simulation leads to the lower correlation to the CT orientation vectors within these samples. In Fig. 7, plots through the thickness of the orientation yy and zz components as well as porosity are given. Values are taken at the middle of the CT specimens and the closest point in the Moldflow mesh. It is probably not only the model resolution that gives the rather low correlation even though the correlation is higher at Sample 3 and 4 where the flow is more stable. It is also noted that the porosity prediction from Moldflow is about 2 times lower that what is measured in the CT analysis. To give further comparison, a density measurement was done on a sample extracted at location 3 from a different specimen of the same batch (Table 1:) showing a value that is significantly lower than from the CT scan.

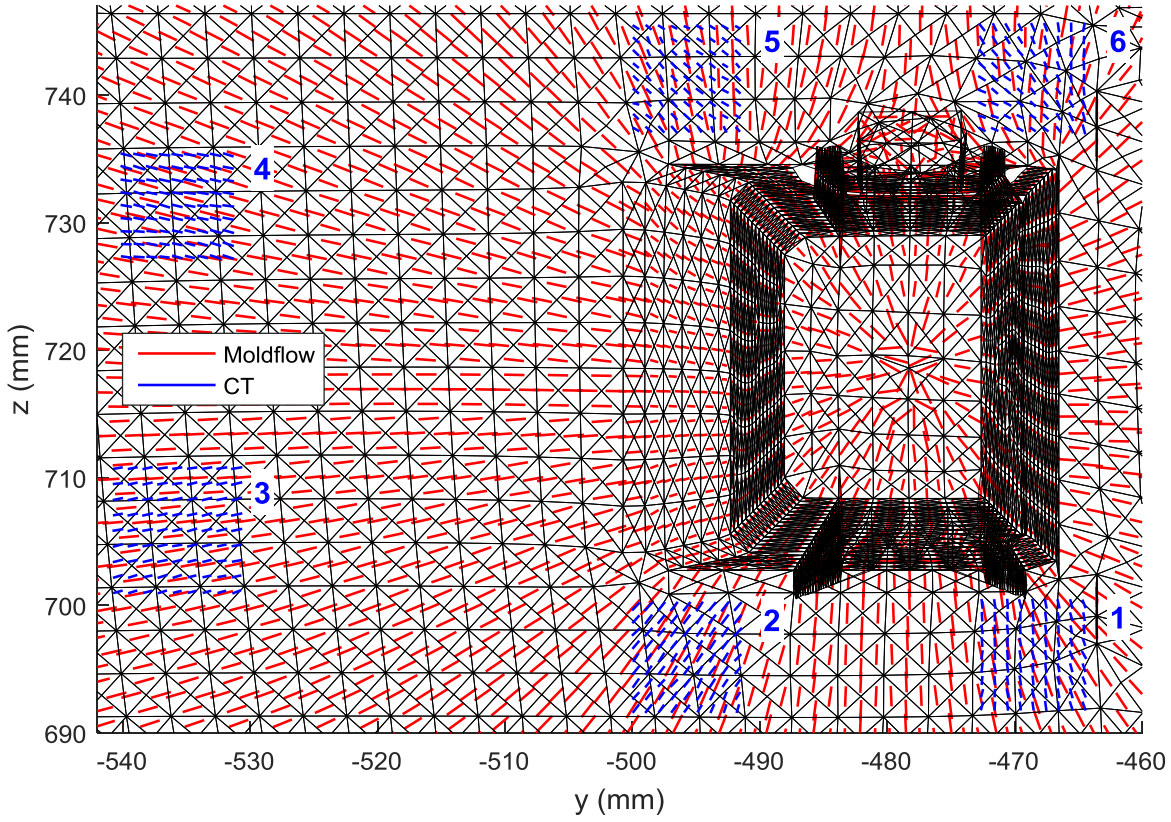

Fig.6: Plot of first eigenvector of the fiber orientation tensor at second layer close to the surface. Data from CT specimens extracted from six locations (1-6) on the component on top of Moldflow mesh and prediction.

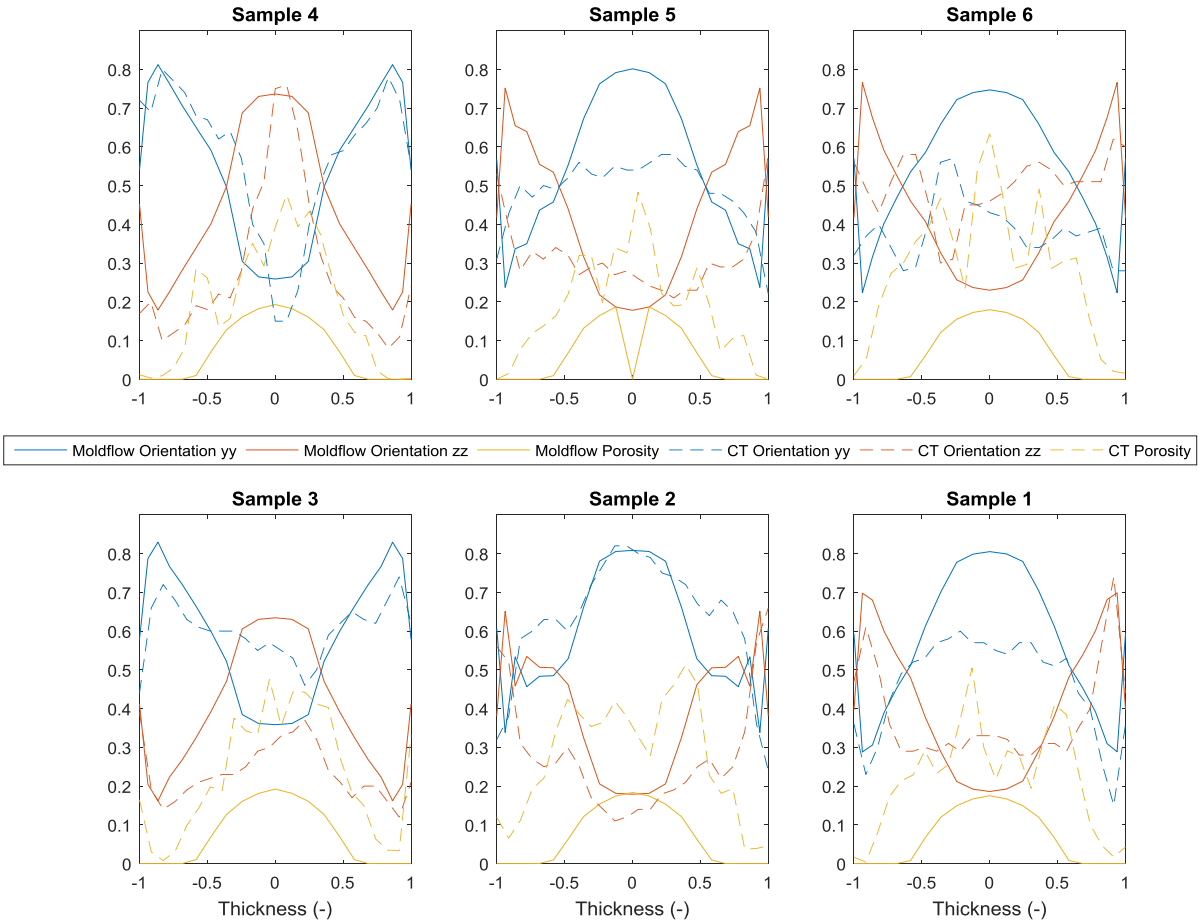

Fig.7: Orientation tensor yy and zz components as well as porosity at midpoint of samples as a function of relative thickness. Moldflow predictions and calculations from CT reconstruction.

Sample	1	2	3	4	5	6
Model thickness	2.45	2.45	2.45	2.45	2.45	2.45
CT thickness	2.26	2.25	2.27	2.25	2.30	2.20
Moldflow Porosity %	7.7	7.3	7.6	7.6	7.7	7.7
CT Porosity %	22.5	23.4	19.5	16.8	16.5	27.5
DM porosity %	-	-	10.3	-	-	-
CT Fiber fraction %	29.0	29.4	34.3	39.7	37.8	28.0

Table 1: Model (Moldflow and LS-DYNA) thicknesses, thicknesses of the volume analyzed in CT, average porosity prediction from Moldflow, average porosity from CT, porosity based on density measurement and average fiber fraction from CT for all six samples.

5 Validation of impact response

5.1 Testing

For the validation of the final CAE model for impact analysis, drop testing in two directions was performed. The support fixture, green polyurethane in Fig. 8, was custom CNC machined to have the same surface as the bumper cover to provide good support of the combined bracket. Additionally, bolts were used to clamp the bracket to the surface. In the legform to bumper tests (Section 2), force is transferred from the bumper cover to the cone which has strong support from the side members. In the test loadcases, the force is instead introduced by the impact on the cone leading to a loading that is close to the one in the legform test. The tests were performed at a variation of impact velocities ranging from low speed where no cracks were visible after the test to higher speed where clear cracks were sustained. Fig. 9 and Fig. 10 show the failure sustained at the tests.

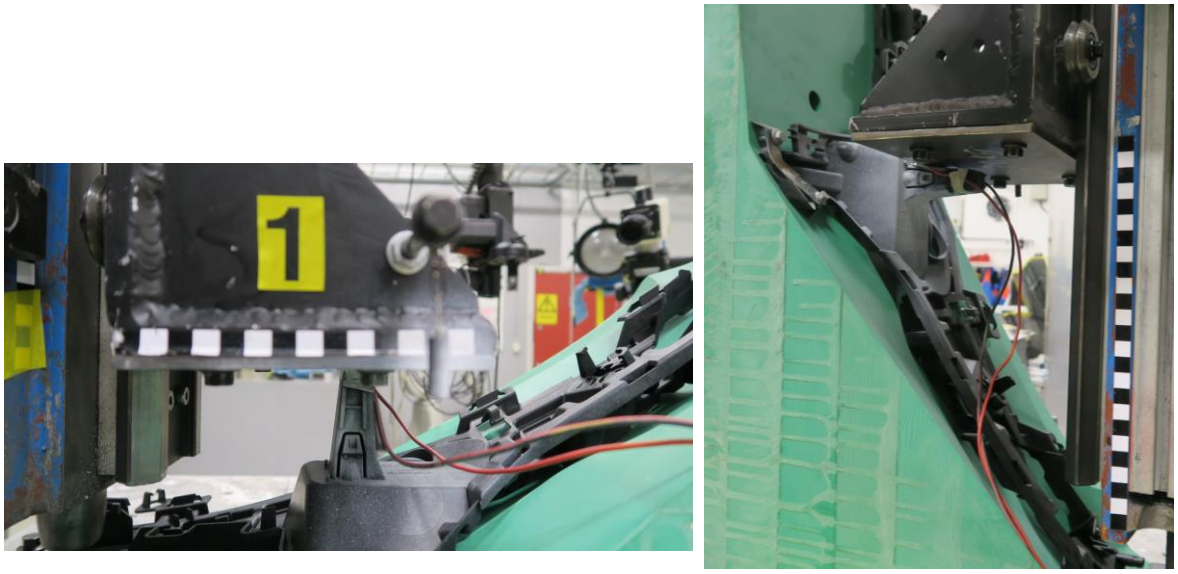

(A) (B)

Fig.8: Test loadcase A: axial loading and B: transverse loading.

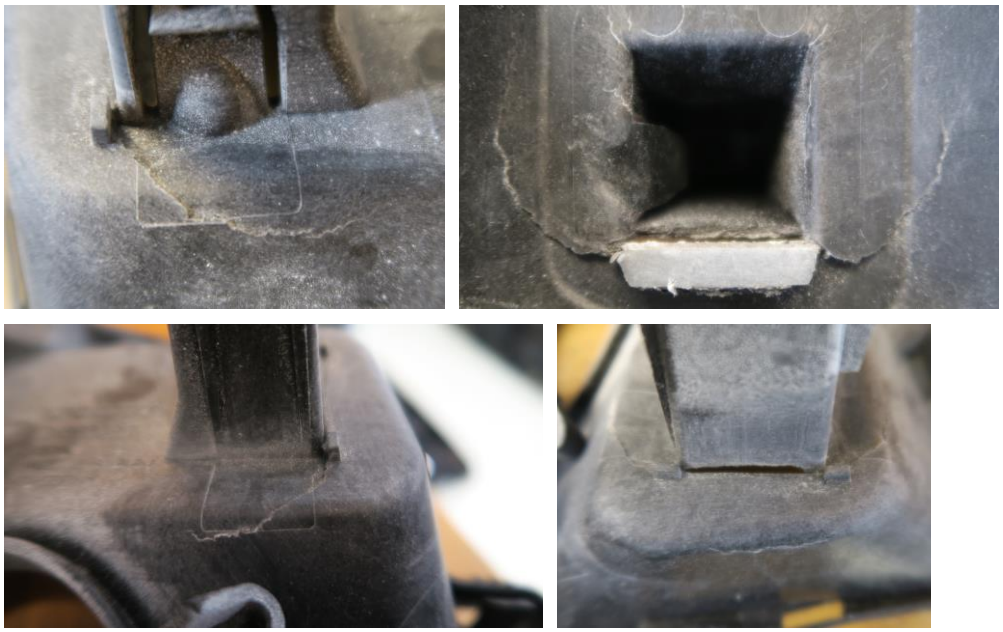

Fig.9: Failure mode sustained in loadcase A.

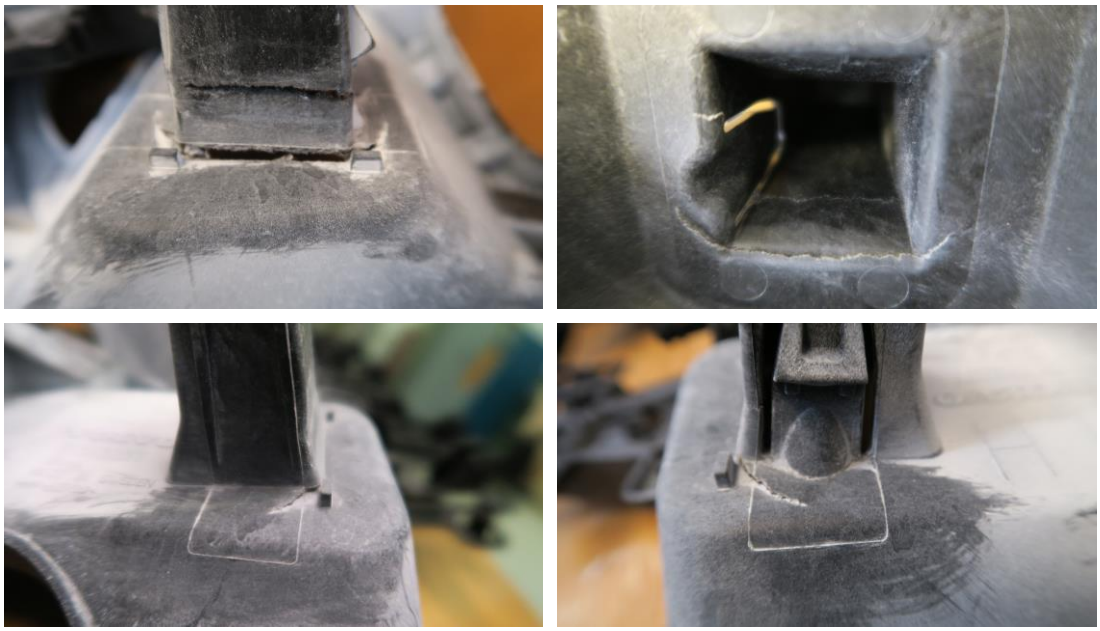

Fig.10: Failure mode sustained in loadcase B.

5.2 Simulations

The simulations were done in LS-DYNA using the same shell model that is used for safety assessment in the development of the vehicle. The elements have the side length of about 3 mm. The material model is DIGIMAT version 2019.0 [1] elastoviscoplastic with Tsai-Hill 3D transversely isotropic pseudo grain failure calibrated as described in Section 3. The model uses a von Mises symmetric yield surface and is calibrated in tension only. However, to avoid early failure in compression a scaling is applied. The scaling of the failure strains starts at 1 for positive stress triaxiality and increases linearly to a chosen value for hydrostatic stress state. The value of the factor was chosen to 10 in this case. An additional model parameter is the number of integration points required to fail for the element to erode. This parameter was set for the element to erode at failure of all integration points.

In Fig. 11, we can observe the effect of the porosity in the material model. As we include the effect of porosity, the amount of failure is highly over-estimated while the porosity effect on the stiffness seems to be correct. Based on this result it was determined that the model without pososity including failure was the most suitable one.

Fig.12 shows energy-displacement curves for the two loadcases at two impact velocities each. For the lower impact velocity in each loadcase, no fractures are visible after the test. This is well reproduced in loadcase B, see Fig. 14. In loadcase A, however, the model predicts failure also at the lower velocity (Fig. 13). For the stiffness during the loading phase, we have a very good agreement in loadcase A while in loadcase B we lose too much stiffness during the second half of the loading phase. When it comes to the unloading phase, the results indicate that too much energy is dissipated in plasticity. This could point towards a viscoelastic-viscoplastic model being more suitable for the application. A viscoelastic-viscoplastic model is indeed available in DIGIMAT but it has not been applied in the current case.

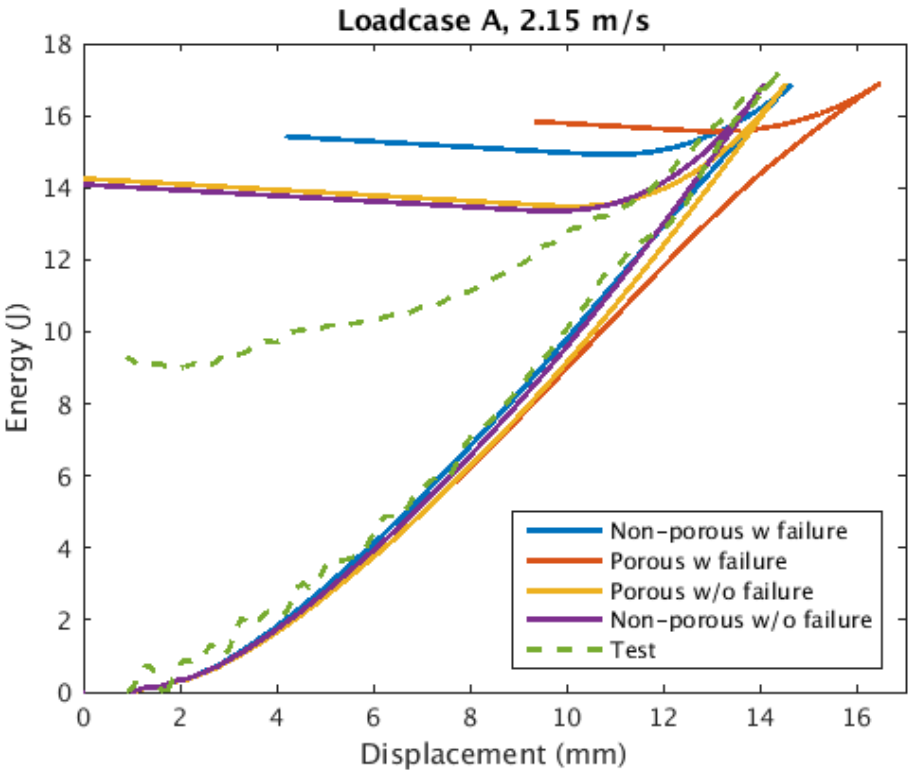

Fig.11: Results from loadcase A at 2.15 m/s impact speed in terms of energy as function of displacement. Results from test and simulations with four different material models: non-porous with failure, porous with failure, porous without failure and non-porous without failure.

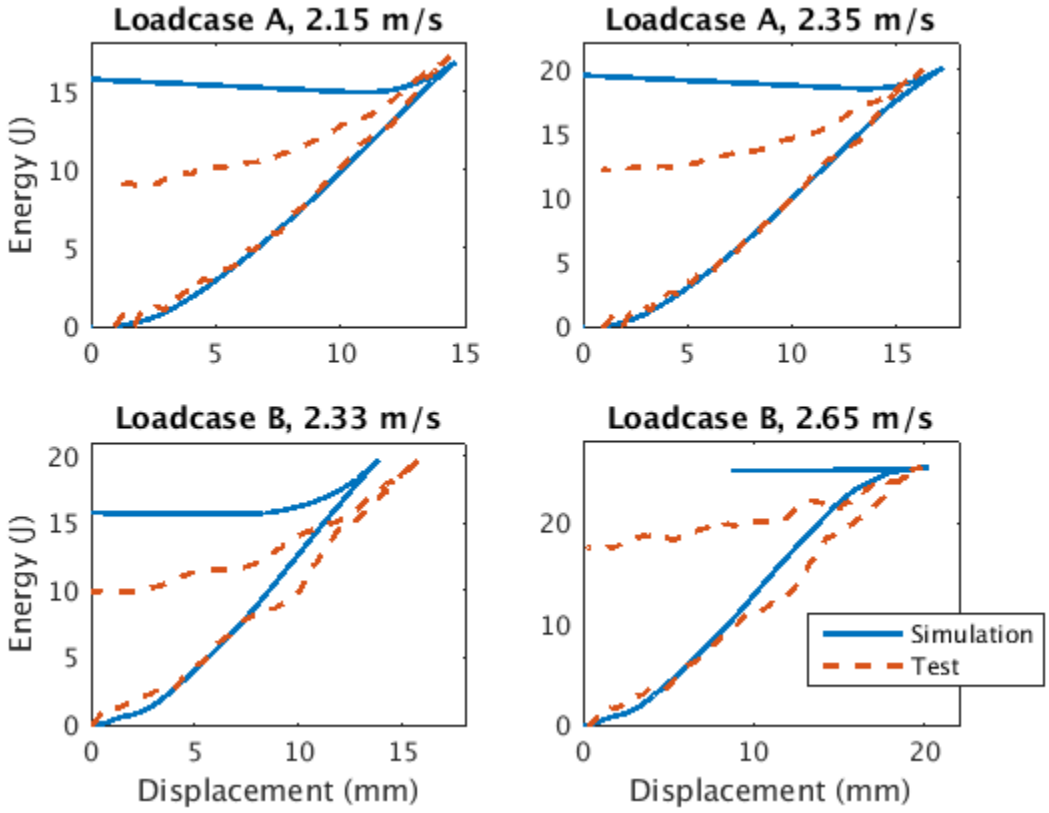

Fig.12: Energy versus displacement for loadcase A at 2.15 and 2.35 m/s impact speed and for loadcase B at 2.33 and 2.65 m/s.

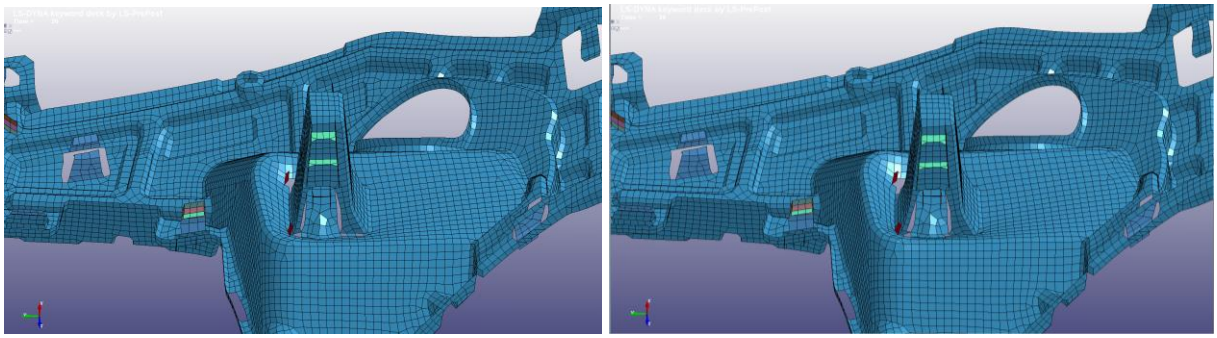

Fig.13: Simulation model of loadcase A at 30 ms after initial impact. Impact velocity 2.15 and 2.35 m/s, respectively.

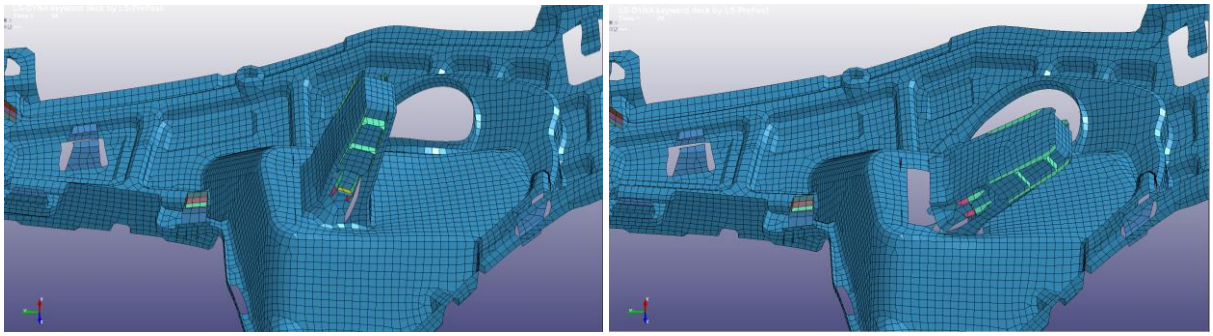

Fig.14: Simulation model of loadcase B at 30 ms after initial impact. Impact velocity 2.33 and 2.65 m/s, respectively.

6 Conclusions

The DIGIMAT material model using Moldflow predictions of fiber orientation was applied for a microcellular PPGF30 component in impact analysis. The agreement to physical test is good considering the model detail level and the required input data. Potentially improvements of failure prediction can be made from solid modeling [14] and a failure model with a direct dependency of stress triaxiality. The latter is since recently available in DIGIMAT. It will, however, require additional material test data. Including the effect of porosity in the material modeling gives the expected small reduction of stiffness and a larger unexpected reduction of the toughness. Further investigations on how porosity influences the failure in the model are suggested. In the present paper, the effect of porosity was removed.

To assess quality of the predictions of fiber orientation and porosity, CT scanning was done. Comparisons show discrepancies between CT and Moldflow data. The details of the Moldflow analysis have nevertheless not been investigated further.

7 Acknowledgements

Colleagues at Volvo Cars are acknowledged for their contributions, especially Kai Kallio, Material Centre, for organizing the CT scan and making the density measurement. Anoop Ravi at Plastal Industri AB is acknowledged for doing the Moldflow analysis. Hédi Skhiri, Maxime Melchior and colleagues at e-Xstream are acknowledge tor their support.

8 Literature

[1] DIGIMAT: www.e-xstream.com
[2] Landervik, L and Jergeus, J: “Digimat Material Model for Short Fiber Reinforced Plastics at Volvo Car Corporation”, 10th European LS-DYNA Conference, Würzburg, 2015
[3] Foss, P: “Prediction of the Drop Impact Performance of a Glass Reinforced Nylon Oil Pan”, 13th International LS-DYNA Users Conference, Detroit, 2014

[4] Sakakibara, T et al: "Simulation of Ball Impact on Composite Plate with PP+30% LGF", 12th International LS-DYNA Users Conference, Detroit, 2012
[5] Reithofer, P et al: "*MAT_4A_MICROMEC – Theory and Application notes", 15th International LS-DYNA Conference, Detroit, 2018
[6] Liebold C, Erhart, A and Haufe, A: “The Significance of the Production Process of FRP Parts for the Performance in Crashworthiness”, 14th International LS-DYNA Conference, Detroit, 2016
[7] Liebold C and Haufe, A: “process2product simulation: Closing Incompatibilities in Constitutive Modeling and Spatial Discretization with envyo®", 15th International LS-DYNA Conference, Detroit, 2018
[8] LS-DYNA R11 Keyword User's Manual, Volume II: Material Models, LSTC, 2018
[9] Gómez-Monterde, J et al: "Microcellular PP/GF composites: Morphological, mechanical and fracture characterization", Composites: Part A, 104, 2018, 1–13
[10] Elduquea, D et al: "Methodology to Analyze the Influence of Microcellular Injection Molding on Mechanical Properties with Samples Obtained Directly of an Industrial Component", Polymers & Polymer Composites, 22 (8), 2014, 743–752
[11] Wetzstein, I et al: "Optimization of a Lower Bumper Support regarding Pedestrian Protection Requirements using ANSA and LS-OPT", 10th European LS-DYNA Conference, Würzburg, 2015
[12] European New Car Assessment Programme (Euro NCAP) Pedestrian Testing Protocol, Version 8.5, 2018
[13] European New Car Assessment Programme (Euro NCAP) Assessment Protocol – Pedestrian Protection, Version 9.0.3, 2018
[14] Brenner, F et al: “Influence of Discretisation on Stiffness and Failure Prediction in Crashworthiness Simulation of Automotive High Pressure Die Cast Components”, 9th European LS-DYNA Conference, Manchester, 2013